AD-A166 443 TELESEISMIC WAVEFORM MODELING INCORPORATING THE EFFECTS 1/1
OF KNOWN THREE-DI..(U) MASSACHUSETTS INST OF TECH
CAMBRIDGE EARTH RESOURCES LAB V F CORMIER 22 OCT 85
UNCLASSIFIED AFGL-TR-85-0264 F19628-85-K-0031 F/G 8/11 NL

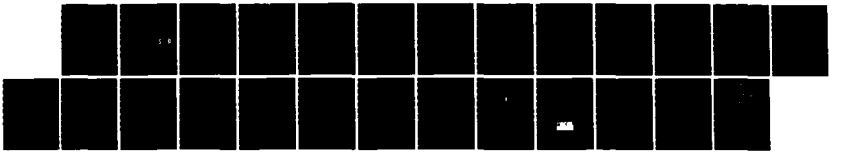

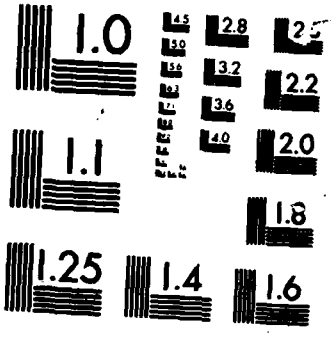

MICROCOPY RESOLUTION TEST CHART

AFGL-TR-85-0264

TELESEISMIC WAVEFORM MODELING INCORPORATING THE EFFECTS OF KNOWN THREE-DIMENSIONAL STRUCTURE BENEATH THE NEVADA TEST SITE

Vernon F. Cormier

Massachusetts Institute of Technology
Earth Resources Laboratory
Department of Earth, Atmospheric, and
Planetary Sciences
Cambridge, MA 02139

22 October 1985

Scientific Report No. 1

AIR FORCE GEOPHYSICS LABORATORY
AIR FORCE SYSTEMS COMMAND
UNITED STATES AIR FORCE
HANSCOM AIR FORCE BASE, MASSACHUSETTS 01731

CONTRACTOR REPORTS

This technical report has been reviewed and is approved for publication.

JAMES F. LEWKOWICZ
Contract Manager

HENRY A. OSSING
Chief, Solid Earth Geophysics Branch

FOR THE COMMANDER

DONALD H. ECKHARDT
Director
Earth Sciences Division

This report has been reviewed by the ESD Public Affairs Office (PA) and is releasable to the National Technical Information Service (NTIS).

Qualified requesters may obtain additional copies from the Defense Technical Information Center. All others should apply to the National Technical Information Service.

If your address has changed, or if you wish to be removed from the mailing list, or if the addressee is no longer employed by your organization, please notify AFGL/DAA, Hanscom AFB, MA 01731. This will assist us in maintaining a current mailing list.

REPRODUCED AT GOVERNMENT EXPENSE

DISCLAIMER NOTICE

THIS DOCUMENT IS BEST QUALITY PRACTICABLE. THE COPY FURNISHED TO DTIC CONTAINED A SIGNIFICANT NUMBER OF PAGES WHICH DO NOT REPRODUCE LEGIBLY.

unclassified

SECURITY CLASSIFICATION OF THIS PAGE (When Data Entered)

REPORT DOCUMENTATION PAGE		READ INSTRUCTIONS BEFORE COMPLETING FORM
1. REPORT NUMBER AFGL-TR-85-0264	2. GOVT ACCESSION NO. AD-A166 443	3. RECIPIENT'S CATALOG NUMBER
4. TITLE (and Subtitle) Teleseismic Waveform Modeling Incorporating the Effects of Known Three-Dimensional Structure Beneath the Nevada Test Site		5. TYPE OF REPORT & PERIOD COVERED Technical Report No. 1 2/4/85-7/31/85 6. PERFORMING ORG. REPORT NUMBER
7. AUTHOR(s) Vernon F. Cormier		8. CONTRACT OR GRANT NUMBER(s) F19628-85-K-0031
9. PERFORMING ORGANIZATION NAME AND ADDRESS Earth Resources Laboratory, Dept. of Earth, Atmospheric, and Planetary Sciences, M.I.T., Cambridge, MA 02139		10. PROGRAM ELEMENT, PROJECT, TASK AREA & WORK UNIT NUMBERS 61101E 5A10DAAJ
11. CONTROLLING OFFICE NAME AND ADDRESS Air Force Geophysics Laboratory Hanscom AFB, Massachusetts 01731 J. Lewkowicz/LWH		12. REPORT DATE 10/22/85 13. NUMBER OF PAGES 24
14. MONITORING AGENCY NAME & ADDRESS(if different from Controlling Office)		15. SECURITY CLASS. (of this report) unclassified 15a. DECLASSIFICATION/DOWNGRADING SCHEDULE

16. DISTRIBUTION STATEMENT (of this Report)

Approved for public release; distribution unlimited

17. DISTRIBUTION STATEMENT (of the abstract entered in Block 20, if different from Report)

18. SUPPLEMENTARY NOTES

19. KEY WORDS (Continue on reverse side if necessary and identify by block number)

seismic body waves, three-dimensional structure, ray tracing, synthetic seismograms

20. ABSTRACT (Continue on reverse side if necessary and identify by block number)

Seismograms were synthesized by the Gaussian beam method and ray trajectories were plotted for a plane wave incident on a 3-D structure obtained from block inversion of teleseismic travel times observed at a local array in central California. The amplitude variations for the given profile are smaller than the order of magnitude variations typically observed. Since amplitudes are sensitive to smaller scale velocity features than travel times, this may indicate that a single scale block model may have difficulty in satisfying both travel time and amplitude.

DD FORM 1 JAN 73 1473 EDITION OF 1 NOV 65 IS OBSOLETE

unclassified

SECURITY CLASSIFICATION OF THIS PAGE (When Data Entered)

(20. continued)

CONT

The synthesis of teleseismic body waves by either the Gaussian beam, Maslov, or Kirchhoff techniques entails the integration of dynamic and kinematic ray tracing equations over parts of the model having 3-D as well as 1-D velocity variations. The longest integration intervals are over the 1-D or radially symmetric part of the model. A procedure consisting of the multiplication of propagator matrices can be used to smoothly patch analytic solutions of the dynamic equations obtained over the 1-D or radially symmetric part of the model into numerical solutions obtained over the parts of the model having 3-D velocity variations.

SUMMARY

Seismograms were synthesized by the Gaussian beam method and ray trajectories were plotted for a plane wave incident on a 3-D structure obtained from block inversion of teleseismic travel times observed at a local array in central California. The amplitude variations for the given profile are smaller than the order of magnitude variations typically observed. Since amplitudes are sensitive to smaller scale velocity features than travel times, this may indicate that a single scale block model may have difficulty in satisfying both travel time and amplitude.

The synthesis of teleseismic body waves by either the Gaussian beam, Maslov, or Kirchhoff techniques entails the integration of dynamic and kinematic ray tracing equations over parts of the model having 3-D as well as 1-D velocity variations. The longest integration intervals are over the 1-D or radially symmetric part of the model. A procedure consisting of the multiplication of propagator matrices can be used to smoothly patch analytic solutions of the dynamic equations obtained over the 1-D or radially symmetric part of the model into numerical solutions obtained over the parts of the model having 3-D velocity variations.

1. INTRODUCTION

Observations of teleseismic P waves at large aperture arrays have found amplitude fluctuations across the array as large as those observed over the world wide networks. The amplitude fluctuations and their correlation with travel time variations are consistent with the focussing/defocussing effects of three-dimensional velocity structure beneath the array rather than the effects of intrinsic attenuation. In this semi-annual report, the Gaussian beam method is used to predict the possible amplitude variations at a large aperture array due to a known 3-D structure The known 3-D structure is determined from a block-inversion of travel times of the type described by Aki et al. (1976). For body waves on the order of 1 Hz. dominant frequency, the scale length and intensity variations of the models commonly derived from such inversions are well within the bounds in which asymptotically approximate methods, such as the Gaussian beam method, are valid.

A goal of these experiments is to determine whether knowledge of the 3-D structure surrounding a given nuclear test site can be used to reduce the uncertainty in a yield estimate by providing an amplitude correction that is a function of source location within the test site. Although the spatial resolution of 3-D block inversions is much less than that obtainable from on-site reflection experiments and well-logs, it is a less intrusive experiment. Such inversions are always possible if the events within a test site are well timed and located. Thus it is important (1) to determine whether the spatial resolution of 3-D block inversions is sufficient to explain any significant amplitude variations in teleseismic P waves due to variations of event locations within a test site and (2) to determine the relation between characteristic scale lengths and intensities of velocity fluctuations of these models with predicted amplitude fluctuations.

The preliminary calculations shown in this report have approximated the effects of velocity variations beneath a test site by the reciprocal problem of a plane wave front

incident on a three-dimensionally varying structure. In order to more precisely calculate the teleseismic problem, it is necessary to determine the geometric spreading and Gaussian beam amplitudes over long distances through parts of the model that are likely to have much weaker velocity fluctuations. These parts of the model can be represented by a 1-D or radially symmetric earth. In these parts of the model, dynamic ray tracing and quantities needed for Gaussian beam or Maslov synthesis can be rapidly calculated using a propagator matrix technique. Section 4 of this report gives analytic forms for the elements of this propagator in a 1-D earth model.

2. THE GAUSSIAN BEAM METHOD OF SEISMOGRAM SYNTHESIS

The Gaussian beam method is an extension of the ray method for the computation of seismograms in a smoothly varying heterogeneous medium (see Červený et al., 1982). In comparison to other methods, the Gaussian beam method is fast, gives finite amplitudes at caustics, and requires no explicit two-point ray tracing. The method uses rays as a framework upon which the wavefield is built. The Gaussian beams are propagated along each ray and then superposed at the receiver. The beams are weighted in the superposition in order to satisfy a given source condition.

The individual beams in the superposition can be manipulated by a complex beam parameter which changes the beam curvature and beam width at the source. This is done in order to satisfy different objectives, such as small beam width at the source, receiver, or at a localized heterogeneity, or to satisfy a given curvature condition. It has been found that large initial beam widths are more suitable for the decomposition of a point source into Gaussian beams and small initial beam widths are more suitable for the decomposition of a plane wave into Gaussian beams (see Nowack and Aki, 1984). The Gaussian beam method reduces to a plane wave expansion for large planar beams at a point source in a homogeneous source region. Finite beam widths have the effect of localizing the beams to a vicinity of each central ray, and reducing numerical end effects in the superposition (see Madariaga and Papadimitriou, 1985). Finite beam

widths also reduce diffraction effects in certain cases, such as the generation of a head wave at a plane interface. The critical initial beam width gives the beam solution most concentrated about each central ray and is a compromise that has been found to give stable results. Tests at a simple caustic have nonetheless given the correct behavior over a range of initial beam widths. More work must be done, particularly in 1-D and 2-D, in choosing the appropriate beam parameter that gives the best results for a given heterogeneous medium.

The numerical advantages of using high frequency asymptotic methods are most pronounced in three-dimensional cases. The finite difference method in contrast is slow for 2-D wave propagation problems, and impractical for most 3-D seismic wave problems. Still, many problems require approximate 3-D solutions. It is thus of interest to develop asymptotic methods such as the Gaussian beam method for the 3-D case.

3. RESULTS WITH A 3-D MODEL

An example 3-D structure can be obtained from a model determined from a travel time inversion parameterized by blocks or by any other method. Here, the results from a teleseismic travel time inversion study for central California by Zandt (1981) are used. The model has four layers from 0.0 to 90.0 km in depth. The horizontal block size is 10.0 km in the top layer and 20.0 to 25.0 km in the lower layers. Average velocity variations in the derived model are between 4.0 to 8.0 percent in the top layer and 2.0 to 4.0 percent in the lower layers. Comer and Aki (1982) investigated this structure using 3-D ray tracing in order to study the effect of ray bending on estimated take-off angles for shallow events. Figure 1a shows an example of down going rays from a shallow event in the central California structure. The 3-D ray tracer used is a modification of a subroutine written by R. Comer. The velocity model is interpolated using a 3-D splines under tension package by A. Cline. Figure 1b shows a top view of the ray paths in which ray bending can clearly be seen. The rays associated with a teleseismic plane wave incident from below is shown in Figure 2a. A more dense set of

rays is shown in Figure 2b. Again, ray bending can be seen in the ray diagrams.

To compute synthetic seismograms, the paraxial ray equations must be solved along each ray. These equations are a linearized set of equations which can be used to obtain information in the vicinity of a ray that has already been traced using the kinematic ray equations. The paraxial (dynamic) ray equations are useful in a variety of ways including the computation of geometric spreading and amplitude in the standard ray method, the calculation of local wave front curvature for phase interpolation, and the computation of polarization vectors, etc. (see Červený, 1985a). Complex solutions of these equations are used in the Gaussian beam method. Thus, once the kinematic and paraxial ray equations are solved in the vicinity of the receiver, this information can be input directly into a Gaussian beam synthesis program.

As an example, Gaussian beam synthetics are computed for the teleseismic plane wave incident from below in the central California model. The endpoints of the rays are shown in Figure 3a. A 2.0 Hz Gabor wavelet is used as the source time function, and a critical initial beam width is used. A correlation between lower amplitudes and earlier arrivals can be seen on the synthetics. The lower amplitude can be identified on Figure 3a near the point A, where the rays are being pulled apart. In Figure 3b, the amplitude varies by a factor of about 2 along the profile. Observations of amplitude at the Montana LASA by Aki (1973) showed variations in the amplitude by a factor of 10. This difference in the amplitude variation may be related to the block sizes used to satisfy the travel time data for the inverted block model. Since travel time is related to the velocity field and amplitude is related to the second derivative of the velocity field, different heterogeneity scales may be required to satisfy both travel time and amplitude variations.

4. THE PROPAGATOR MATRIX FOR DYNAMIC RAY TRACING

Since the dynamic (paraxial) ray tracing system can be written in the linear form $\frac{d\mathbf{W}}{ds} = \mathbf{S}\mathbf{W}$, it permits the definition of fundamental matrix and propagator matrix solutions. Specifically, Červený (1985a) has defined a 4x4 matrix $\Pi(s,s_0)$ that solves this linear system by four linearly independent solutions, with s denoting a point along the ray path where the integration terminates and s_0 a reference point (e.g., source point, receiver point) where the integration starts and initial conditions are specified. Π has the property that $\Pi(s_0,s_0) = \mathbf{I}$, where $\mathbf{I}$ is the identity matrix. Also, given a point s' between s_0 and s, $\Pi(s,s_0) = \Pi(s,s')\,\Pi(s',s_0)$. This property can be used to accelerate two point ray tracing and the calculation of spreading functions and dynamic quantities needed for synthesis of body waves in three-dimensionally varying media by the Gaussian beam and Kirchhoff techniques. For example, if the three-dimensional variations of a model are confined only to the portion of the ray path between s' and s_0, numerical integration of the linear system need only be performed between s_0 and s' to construct $\Pi(s',s_0)$. Along the segment of the ray path between s' and s, traversing a 1-D or homogeneous portion of the model, analytic solutions exist for $\Pi(s,s')$. Thus $\Pi(s,s_0)$ can be simply obtained by multiplying the analytic and numerically obtained Π matrices.

The Π matrix can be defined in terms of 2 x 2 sub matrices $\mathbf{P}$ and $\mathbf{Q}$ as follows:

$$\Pi = \begin{bmatrix} \bar{\mathbf{Q}} & \mathbf{Q} \\ \bar{\mathbf{P}} & \mathbf{P} \end{bmatrix} \tag{1}$$

where the bar over $\mathbf{Q}$ and $\mathbf{P}$ distinguishes plane wave solutions from point source solutions to the dynamic ray tracing equations. The dynamic ray tracing equations are

$$\frac{d\mathbf{Q}}{ds} = v\mathbf{P} \tag{2a}$$

and

$$\frac{d\mathbf{P}}{ds} = -v^{-2}\nabla v\,\mathbf{Q} \tag{2b}$$

where

$$\mathbf{V} = \begin{bmatrix} -v^{-2}v_{11} & -v^{-2}v_{12} \\ -v^{-2}v_{21} & -v^{-2}v_{22} \end{bmatrix}$$

The subscripts on the elements of **V** denote differentiation of velocity v with respect to the ray centered co-ordinate directions q_1 and q_2. In order to determine the elements of the Π matrix, one must first select a vector basis of the ray centered co-ordinate system (q_1, q_2, t) at the point at which itial conditions are specified. Here, given a fixed Cartesian co-ordinate system (x, y, z), the ray will be assumed to be confined to the (y,z) plane in a 1-D medium and the e_1 direction will be chosen to point in the y direction. A vector e_2 is chosen such that (e_1, e_2, t) forms an orthogonal, right-handed vector basis, where t is the ray tangent.

With this definition of the ray centered co-ordinate system, and assuming that velocity varies only as a function of z (1-D medium), it is possible to derive analytic expressions for the elements of Π. The solutions for the spreading of a line source in a vertically (z) varying medium have been given by Madariaga (1984). These are appropriate for the 22 components of the **Q** and **P** matrices. For the spreading of a point source in three dimensions, solutions for the 11 components must be added to these. The 11 components are quite simple in form. This is because by the choice of the ray centered co-ordinates in the 1-D medium, $v_{11} = 0$. Also the off diagonal elements of the **Q** and **P** matrices are all zero because the velocity v is assumed not to vary in the x and y directions. In summary, the 16 components of the Π matrix in a vertically varying medium are

$$Q_{11} = P_{11} = 1$$

$$Q_{11} = \frac{X}{p}$$

$$Q_{12} = Q_{12} = P_{11} = P_{12} = P_{12} = Q_{21} = Q_{21} = P_{21} = P_{21} = 0$$

$$\bar{Q}_{22} = \cos\delta\left(\frac{1}{\cos\delta_o} + p^2 v_z^o \frac{dX}{dp}\right)$$

$$Q_{22} = \cos\delta\cos\delta_o \frac{dX}{dp}$$

$$\bar{P}_{22} = \frac{p^2 v_z^o}{\cos\delta}\left(1 - p^2 v_z \cos\delta \frac{dX}{dp}\right) - p^2 \frac{v_z}{\cos\delta_o}$$

$$P_{22} = \frac{\cos\delta_o}{\cos\delta}\left(1 - p^2 v_z \cos\delta \frac{dX}{dp}\right)$$

Using this definition of the propagator Π, it can be verified that for any point s' along the ray path at which the velocity and its first spatial derivatives are continuous, that

$$\mathbf{X}(s) = \Pi(s,s')\cdot\Pi(s',s_o)\cdot\mathbf{X}(s_o) \qquad (3)$$

where $\mathbf{X}(s_o)$ is a 2 x 4 matrix of initial conditions on **P** and **Q** and $\mathbf{X}(s)$ is a 2 x 4 matrix formed from a linear combination of plane wave and point source solutions for **P** and **Q**. For example, one can show that given point source initial conditions at s_o, $\mathbf{X}(s_o) = \begin{bmatrix} 0 & 0 \\ 0 & 0 \\ 1 & 0 \\ 0 & 1 \end{bmatrix}$, that $\mathbf{X}(s) = \begin{bmatrix} \mathbf{Q} \\ \mathbf{P} \end{bmatrix}$, where **Q**, **P** are point source solutions at s, and also that $\Pi(s,s_o) = \Pi(s,s')\Pi(s',s_o)$. Also, using this definition of Π it can be verified that the determinant of Π is constant along the ray path and that det $\Pi = 1$.

If the velocity or its first spatial derivative are discontinous at s', then the jump conditions defined by Červený (1985a) must first be applied to the elements of $\Pi(s',s_o)$ before the multiplication of eq. (3) is performed. For the co-ordinate system chosen and for velocity depending only on z, these jump conditions are

$$Q_{22}^{-} = \frac{\cos\delta^{-}}{\cos\delta^{+}} Q_{22}^{+} \tag{4a}$$

and

$$P_{22}^{-} = \frac{\cos\delta^{+}}{\cos\delta^{-}} P_{22}^{+} + \frac{1}{\cos\delta^{-}\cos\delta^{+}} p^2(\cos\delta^{-} v_z^{+} - \cos\delta^{-} v_z^{-}) Q_{22}^{+} \tag{4b}$$

where the + sign refers to quantities on the incident side of the boundary and the - sign refers to quantities on the transmitted side of the boundary. Thus, computations with the propagator matrix of dynamic ray tracing are not completely analogous to those using the stress-displacement propagator. In the former case, the dynamic ray tracing propagator is discontinuous at first and second order velocity discontinuities, while in the latter case the stress-displacement propagator is continuous at solid-solid boundaries. Nevertheless, the multiplication of dynamic ray tracing propagators is still a useful device for extending solutions for the **P** and **Q** matrices from 2- and 3-D regions, in which it is necessary to numerically integrate the dynamic equations through thick 1-D and homogeneous regions, for which the **P** and **Q** elements are known analytically. The patching of the solution is most conveniently performed at pseudo boundaries at which velocity and its first spatial derivatives are continuous. Patching can be performed at more general boundaries provided that one first uses the jump conditions to correct **P**,**Q** elements to values appropriate for the transmitted side of the boundary.

In order for the Π matrix to have the properties of a propagator, one must use the plane wave initial conditions for $\bar{\mathbf{P}}$, $\bar{\mathbf{Q}}$ of Červený (1985a) rather than the modified plane wave conditions recommended by Madariaga (1984) for a source in a region having a non-zero velocity gradient. The modified initial conditions of Madariaga (1984) were proposed to obtain phase fronts at the source that were equivalent to plane waves. This condition was necessary to stabilize the computation of Gaussian beam seismograms. It also makes Gaussian beam synthesis more closely resemble the process of plane wave

superposition upon which Maslov synthesis (Chapman, 1982) is formulated. Recently, however, Červeny' (1985b) has proposed optimal beam width parameters that are equivalent to plane wave fronts at the receiver. These parameters are optimal in the sense of minimizing the error in the truncation of a beam sum. This choice of beam parameters also addresses the stability problem noted by Madariaga. For a source and receiver both at the surface, Červeny''s optimal beam width parameters are reciprocally equivalent to Madariaga's modified plane wave initial conditions. This can be demonstrated using the propagator matrix of dynamic ray tracing and reciprocal relations between elements of the **P** and **Q** matrices.

5. ITERATIVE PARAXIAL RAY TRACING

As an additional check on Gaussian beam synthetics, it is planned to also construct synthetics using the Kirchhoff integral technique (Haddon and Buchen, 1981; Scott and Helmberger, 1983). In this technique an integral must be evaluated on a reference surface between source and receiver. For heterogeneity near the receiver site, this reference surface is most conveniently selected at the base of the heterogeneity. Numerical integration of the dynamic and kinematic ray tracing equations can be performed in a model of the structure beneath the source site. Analytic forms can be used for the spreading and travel times needed for the long paths in a radially symmetric model between the reference surface and the receiver. It is planned to perform this surface integral by a parameterization of the surface in terms of isochrons (contours of equal arrival time between source and receiver, as described in Haddon and Buchen, 1981). An intermediate step to the determination of isochrons is to densely tabulate travel time from the source point to the reference surface. To perform this it is planned to use an iterative ray tracing technique. In this scheme the paraxial approximation is used to calculate take-off angles of rays connecting the source point with a particular point on the reference surface. This scheme is described

in Červený (1985a), and amounts to estimating the new angles γ_1,γ_2 needed to hit a point by the corrections

$$\begin{bmatrix}\gamma_{1\,new}\\ \gamma_{2\,new}\end{bmatrix} = \begin{bmatrix}\gamma_{1\,old}\\ \gamma_{2\,old}\end{bmatrix} + \begin{bmatrix}\Delta\gamma_1\\ \Delta\gamma_2\end{bmatrix} \tag{5}$$

where

$$\begin{bmatrix}\Delta\gamma_1\\ \Delta\gamma_2\end{bmatrix} = \mathbf{Q}^{-1}\begin{bmatrix}q_1\\ q_2\end{bmatrix}$$

with (q_1,q_2) being vector between the point desired and the point actually hit, measured in component directions of the local ray centered co-ordinate system. With this correction it is possible to shoot a sparse fan of rays onto the reference surface and to interpolate travel times, spreading functions, and take-off angles (needed for the source radiation pattern) between densely spaced grid points. An example of the rapid convergence of eq. 5 is shown in Figure 4 for a 3-D model and initial guesses for the take-off angles.

5. CONCLUSIONS AND FUTURE WORK

A test structure, determined from block 3-D inversion of teleseismic travel times, gave amplitude variations of about a factor of 2 along a 100 km. long profile. The block sizes of the test structure varied from 10 - 20 km. in linear dimension with velocity variations on the order of 2 to 8 per cent.

Future work will be directed toward comparing the amplitude fluctuations predicted by 3-D models having varying degrees of resolution in order to determine the resolution required to obtain significant amplitude corrections. A parallel series of experiments will be conducted on synthetic velocity models constructed to have varying distributions of characteristic scale lengths and velocity fluctuations within the domain of validity of the Gaussian beam method.

Synthetics will be constructed at teleseismic distances using beam superposition, ray theory, and the Kirchhoff integral technique. A key step in these calculations will be the patching of dynamic solutions between 1-D and 3-D portions of the earth model using the propagator matrix of dynamic ray tracing. This will enable 3-D model variations to be easily included at both the source and receiver ends of the ray paths. Thus the combined effects on amplitudes of source and receiver structures can be examined.

REFERENCES

Aki, K., Scattering of P waves under the Montana LASA, J. Geophys. Res., 78, 1334-1346, 1973.

Aki, K., A. Christoffersson, and E.S. Husebye, Determination of three-dimensional seismic structures of the lithosphere, J. Geophys. Res., 82, 277-296, 1976.

Červený, V. M.M. Popov, and I. Pšenčík, Computation of wavefields in inhomogeneous media - Gaussian beam approach, Geophys. J.R. astron. Soc., 70, 102-128, 1982.

Červený, V., The application of ray tracing to the propagation of shear waves in complex media, in Seismic Exploration, eds. Trietel, S. and Helbig, K., Vol. Seismic Shear Waves, ed. Dohr., G., Geophysical Press, in press, 1985a.

Červený, V., Gaussian beam synthetic seismograms, J. Geophys., 57, in press, 1985b.

Chapman, C.H., Body-wave seismograms in inhomogeneous media using Maslov asymptotic theory, Bull. Seism. Soc. Am., 72, 5277-5917, 1982.

Comer, R. and K. Aki, Effects of lateral heterogeneity near an earthquake source on teleseismic raypaths, Earthquake Notes, vol. 52, no. 1, 1982.

Haddon, R.A.W., and P.W. Buchen, Use of Kirchhoff's formula for body wave calculations in the earth, Geophys. J. R. astron. Soc., 67, 587-598, 1981.

Madariaga, R., Gaussian beam synthetic seismograms in a vertically varying medium, Geophys. J. R. astron. Soc., 79, 589-612, 1984.

Madariaga, R. and P. Papadimitriou, Gaussian beam modelling of upper mantle phases, preprint, 1985.

Nowack, R. and K. Aki, the 2-D Gaussian beam method: testing and application, J. Geophys. Res., 89, 7797-7819, 1984.

Scott, P. and D.V., Helmberger, Applications of the Kirchhoff-Helmholtz integral to problems in seismology, Geophys. J. R. astron. Soc., 70, 237-254, 1983.

Zandt, G., Seismic images of the deep structure of the San Andreas Fault system, central coast ranges, California, J. Geophys. Res., 86, 5039-5052.

FIGURES

Figure 1a. Ray plot of downward propagating rays for a shallow focus event in the Zandt (1981) structure.

Figure 1b. Surface project of the rays shown in Fig. 1a.

Figure 2a. Rays from a teleseismic plane wave vertically incident on the Zandt (1981) structure.

Figure 2b. Same as Fig. 2a; denser ray spacing.

Figure 3a. Ray intersections with the surface for the incident plane wave described in Fig. 2a and 2b.

Figure 3b. Gaussian beam synthetic seismograms along the profile AA' in Fig. 3a.

Figure 4. An example of the convergence of iterative paraxial ray tracing. Side-view and map-view of ray trajectories are shown. In the side projection the target points are at -2.5, -3.5, -4.5, and -5.5 km. along the right hand margin. All targets lie along the (3.0, 0.0) km. co-ordinates of the map-view. Note that even a poor initial guess for the take off angles in the map-view quickly converges to the target point. The target points lie within a 3-D low velocity zone, which perturbs a piecewise vertical gradient model.

Figure 1

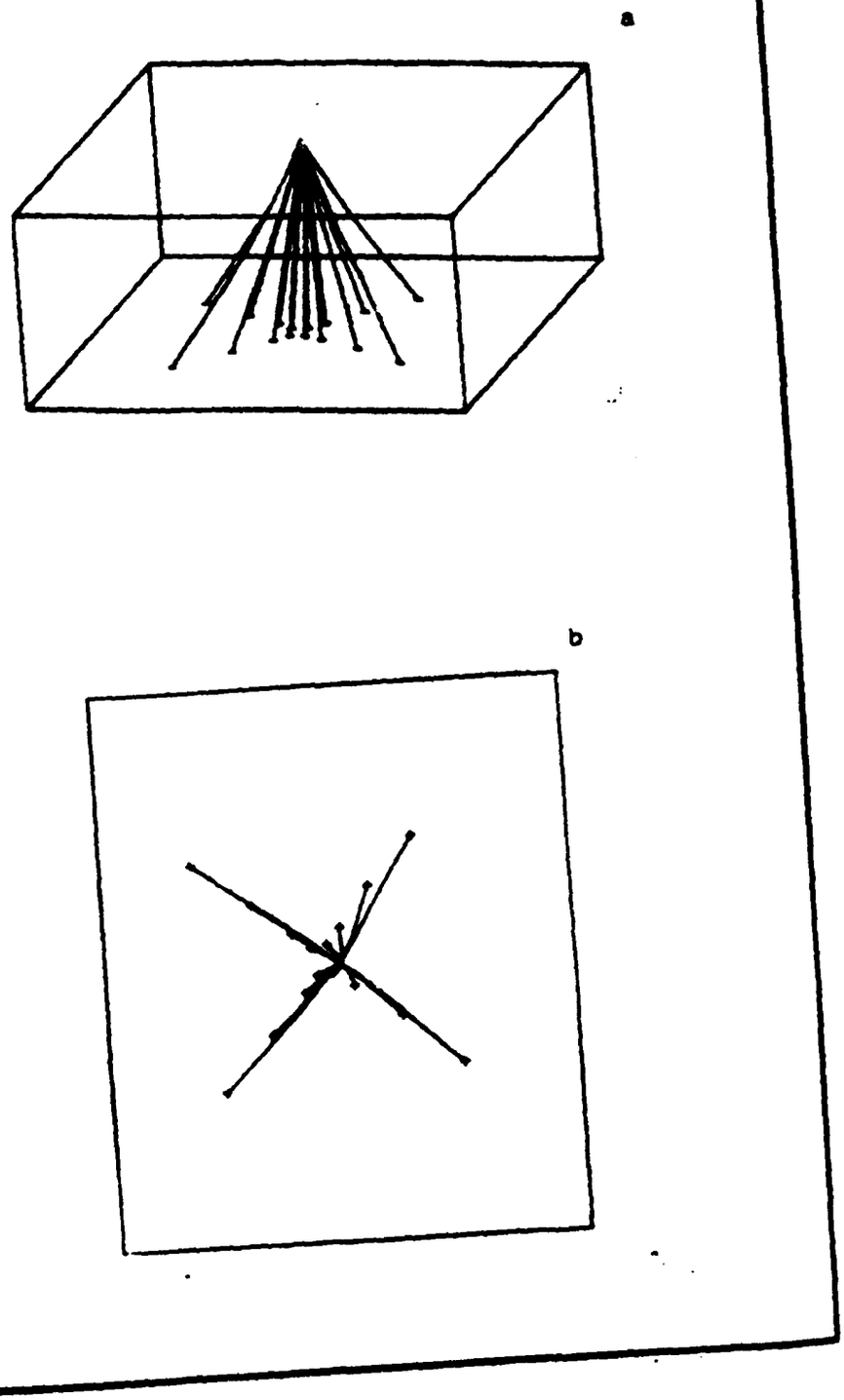

Figure 2

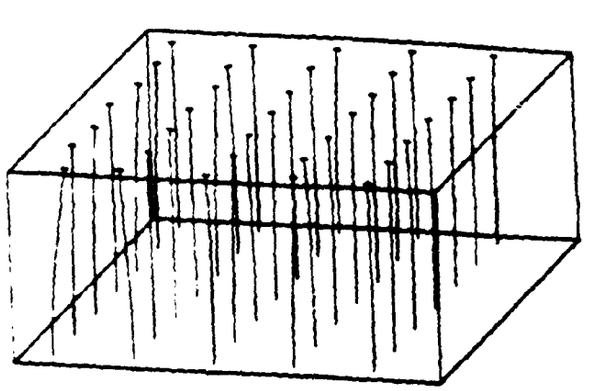

a

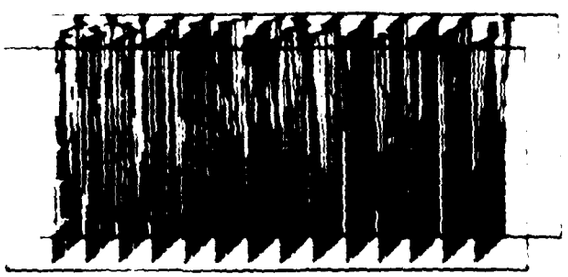

b

Figure 3

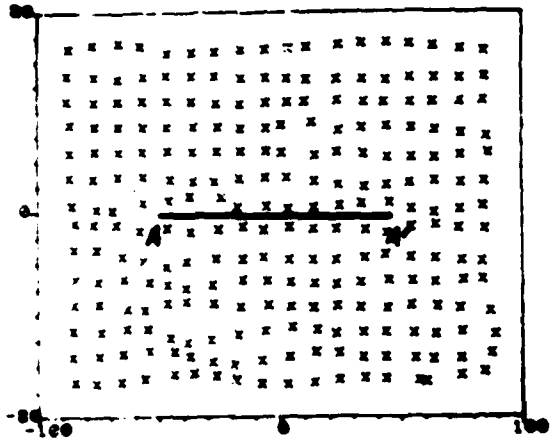

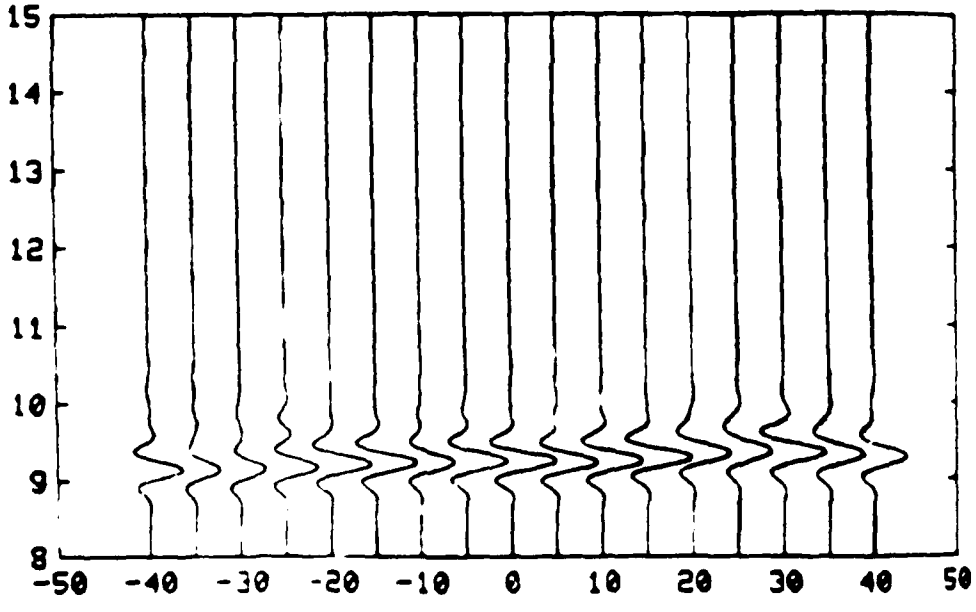

Figure 4

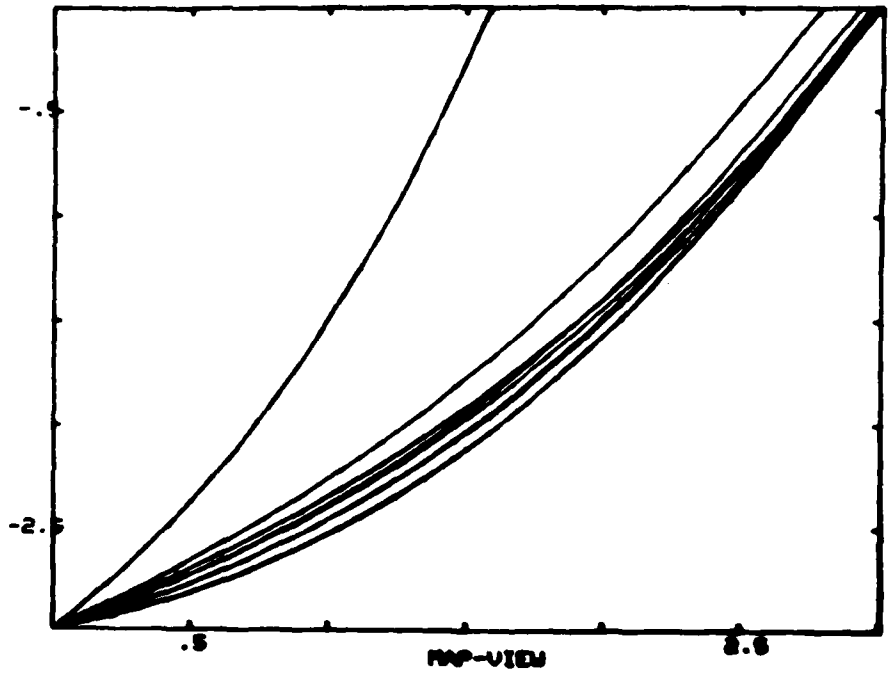

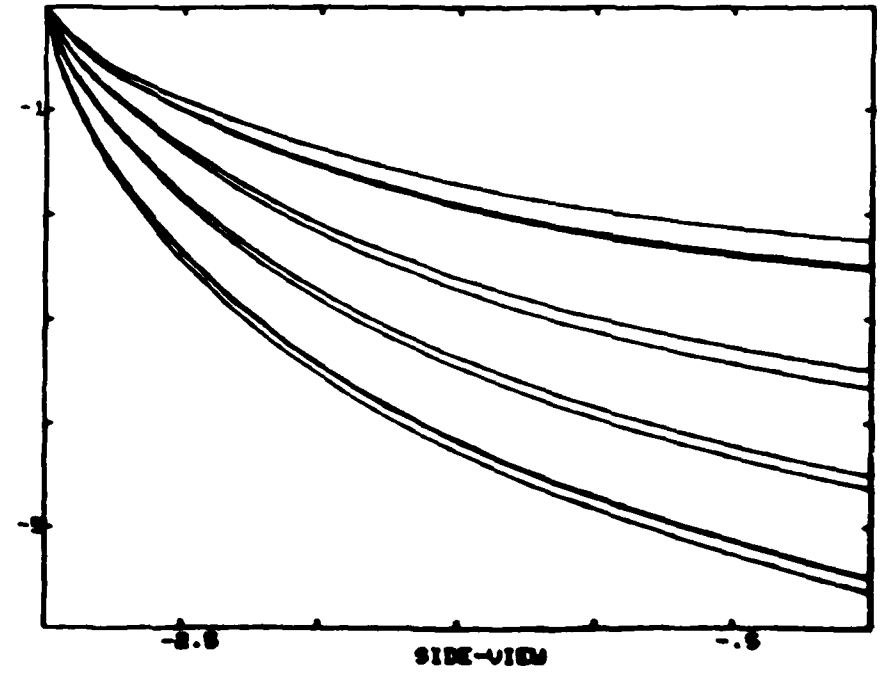

END

FILMED

5-86

DTIC